



## Automated Localisation of Optic Disc and Macula from Fundus Images

**Jaspreet Kaur<sup>1</sup>***ECE&MMU University*  
Jassi3106@gmail.com**Dr.H.P.Sinha<sup>2</sup>***ECE&MMU University*

**Abstract**— Optic disc (OD) detection is a main step while developing automated screening systems for diabetic retinopathy. Optic disc boundary and localization of macula are the two features of retina was necessary for the detection of exudates and also knowing the severity of the diabetic maculopathy. According to the prior information, the diameter of optic disc in a standard retinal image, connected components and iterative thresholding was used to locate optic disc. The macula was localized based on its distance and position with respect to the optic disc as it remained relatively constant. Even though macula is considered to be one of the darkest regions without vessels in a retinal image, less contrast between the macula and background makes it difficult to locate based on image variance. Among 148 images considered for evaluating the methods optic disc and macula were localized with sensitivity of 99.32% and 96.6% respectively. Detection of optic disc boundary becomes important for the diagnosis of glaucoma. Geometric active contour model was explored to segment the optic disc boundary as segmentation algorithms failed to provide good result. Image segmentation was performed by starting with initial curve and evolving its shape by minimizing energy function represented by level set function. The iterative curve evolution was stopped at the image boundaries where the energy was minimum. Experiment was performed on both RGB image and gray scale image and found that implicit active contours provided better result with gray scale images. Total of 74 images were used to evaluate the method. Optic disc boundary drawn manually by an expert was used as ground truth. The method was able to achieve average sensitivity of 90.67% with mean of  $\pm 5.05$ . Based on the result obtained in optic disc boundary detection, it can be stated that geometric based implicit active contour models provide a better segmentation for images with weak boundaries when compared to parametric models.

**Keywords**— Optic disc detection, fovea, image processing, fundus image, diabetic retinopathy

### I. Introduction

An efficient detection of optic disc in colour retinal images is a significant task in an automated retinal image analysis system. Its detection is prerequisite for the segmentation of other normal and pathological features. For instance, the measurement of varying optic disc to cup diameter ratio is used in the detection sight threatening disease called glaucoma. The position of optic disc can be used as a reference length for measuring distances in retinal images, especially for the location of macula. In case of blood vessel tracking algorithms the location of optic disc becomes the starting point for vessel tracking. Finally, in case of diabetic maculopathy lesions identification, masking the false positive optic disc region leads to improvement in the performance of lesion detection.

The attributes of optic disc is similar to attributes of hard exudates in terms of colour and brightness. Therefore it is located and removed during the hard exudates detection process, thereby avoiding false positives. In colour fundus photograph shown in Figure optic disc appears as a bright spot of circular or elliptical shape, interrupted by the outgoing vessels. It can be seen that

optic nerves and vessels emerge in to the retina through optic disc. It is situated on the nasal side of the macula and it does not contain any photoreceptor. Therefore it is also called the blind spot.

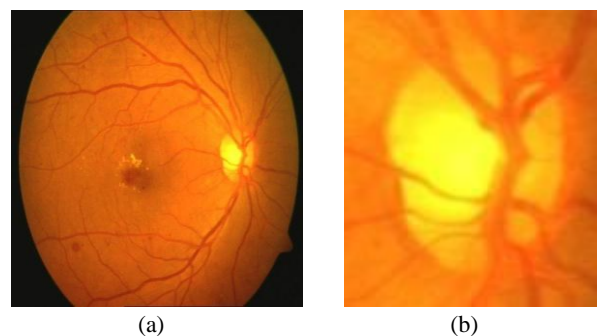


FIGURE 1: Colour retinal image; (a) Optic disc location in the retinal image (b) Enlarged optic disc area

The size of optic disc varies from patient to patient, but its diameter always lies between 80 and 100 pixels in a standard fundus images. There are many factors that make accurate optic disc boundary detection a difficult task. In most of the images the disc boundaries are not clearly visible. And also, several parts of disc will be obscured by the crossing blood vessels. In the current work, the segmentation of optic disc boundary is performed in two steps. First the disc is spatially localized and its approximate center is determined using iterative thresholding and connected component method. This provides a baseline for finding of its exact boundaries. Then, the geometric model based implicit active contour is employed to obtain accurate optic disc boundary. The method was tested on 148 images and qualitatively evaluated by comparing the automatically segmented disc boundaries with manual ones drawn by an experienced ophthalmologist.

## II. Localization of Optic Disc

The localization of optic disc is important for two purposes. First, it serves as the baseline for finding the exact boundary of the disc. Secondly, optic disc center and diameter are used to locate the macula in the image. In a colour retinal image the optic disc belongs to the brighter parts along with some lesions. The central portion of disc is the brightest region called optic cup, where the blood vessels and nerve fibers are absent. Applying a threshold will separate part of the optic disc and some other unconnected bright regions from the background. In this work an optimal thresholding based on Otsu method is applied to separate brighter regions from dark background as follows.

### A. Selection of Initial Threshold

Optimal thresholding method based on approximation of the histogram of an image using a weighted sum of two or more probability densities with normal distribution is used for initial thresholding of the retinal image. Histogram information derived from the source image is used to partition the brightest regions from background. It is observed that disc appears most contrasted in the green channel compared to red and blue channels in the RGB image. Therefore, only the green channel image is used for calculating the optimal threshold. Figure shows the input green channel image and its histogram. It can be seen that the pixels corresponding to the optic disc and the optic cup belong to the higher intensity bars in the histogram. The diameter of the optic disc is in the range of 1.8 to 2mm. Based on the visual inference in a standard retinal image with  $768 \times 576$  size with 20micron/pixel resolution, this prior information is used to calculate the threshold.

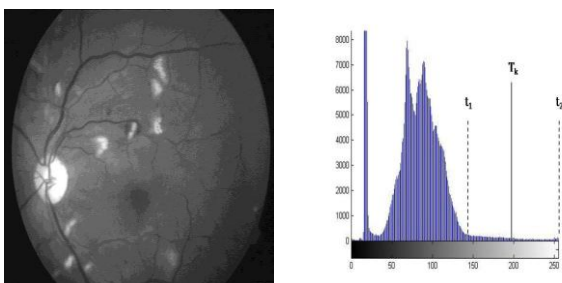


FIGURE 2: Selecting an optimal threshold; (a) Gray scale of green channel retinal image; (b) Corresponding histogram with initial threshold

To obtain an optimal threshold, histogram derived from the source image  $I$  is scanned from highest intensity value  $I_2$  to lower intensity value. The scanning stops at the intensity level  $I_1$  which has atleast a thousand pixels with the same intensity. The initial threshold  $T_k$  for step  $k=1$  is taken as the mean of  $t_2$  and  $t_1$  resulting in subset of histograms. Formulation for the calculation of optimal threshold is given by the following pseudo code.

1. Initial estimate of  $T_k$  is calculated at step  $k$  as

$$T_k = \frac{I_1 + I_2}{2}$$

2. At step  $k$ , apply the threshold. This will produce two groups of pixels:  $G_o$  consisting of all pixels belonging to object region and  $G_b$  consisting of all pixels belonging to background region.

3. Compute the average intensity values and for the pixels in  $G_o$  and  $G_b$  respectively.

4. Update the threshold as follows:

$$T_{k+1} = \frac{\mu_o^k + \mu_b^k}{2}$$

5. Repeat steps 2 through 4 difference in  $T$  in successive iterations is smaller than a predefined value.

Optimal threshold thus calculated results in maximization of gray level variance between object and background. Figure shows the result of thresholding on one of the test image resulting in number of isolated connected regions.

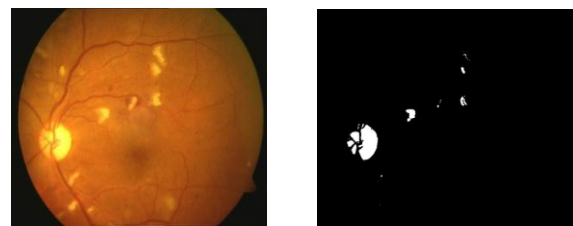


FIGURE 3: Optimal thresholding of retinal image; (a) Input colour retinal image; (b) Thresholded image with number of connected regions.

### B. Estimation of the Optic Disc Center

Thresholding of an image results in number of connected components such as part of optic disc, some noise and other bright features. These connected components are candidate regions for optic disc. The entire image is scanned to count the number of connected components. Each of the connected components in the thresholded image is labeled, total number of pixels in the component and mean spatial coordinates of each connected component is calculated. The component having the maximum number of pixels is assumed to be having the optic cup part of disc and it is considered to be the primary region of interest. The maximum diameter of optic disc can be of 2mm. Therefore, in an image, if any of the components whose mean spatial coordinates are within 50 pixels distance from the mean spatial coordinates of the largest component, then they are merged with it and new mean spatial coordinate is calculated.

Figure illustrates the merging of components if they are part of optic disc.

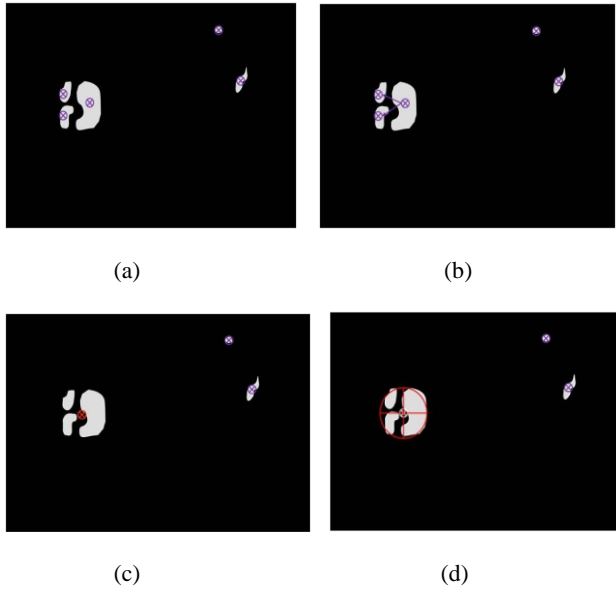


FIGURE 5: Estimating center of optic disc; (a) Candidate regions; (b) Merging of the nearby components into largest component; (c) New centroid of merged region; (d) Ellipse drawn to show the located disc centered at centroid of disc.

If this region is equal to or greater than 1.8mm in diameter an ellipse is drawn to indicate the location of optic disc with its approximate center. Otherwise the threshold is decremented by one and applied to the initial image only in the local rectangular region within the vicinity of the mean spatial coordinates computed earlier. This is to avoid misclassifying lesions as a part of the optic disc. The iterative process is repeated until an optimal size of the optic disc is obtained. The following Figure illustrates the optic disc localization through iterative process and its center estimation.

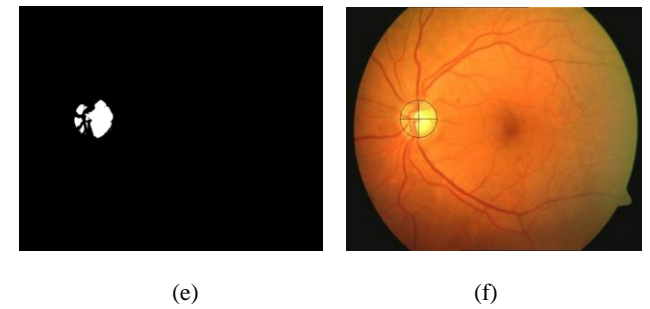
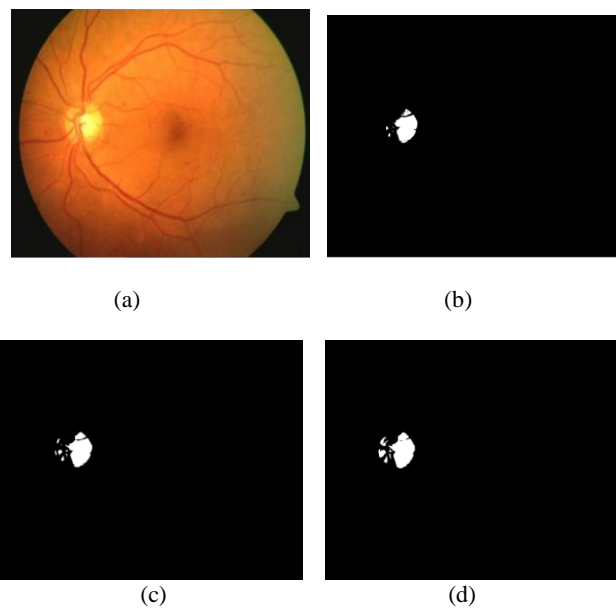


FIGURE 6: Localization of optic disc; (a) Input colour retinal image; (b) Initial thresholding; (c)-(e) Detection phase; (f) Ellipse drawn to show location of optic disc.

### III. optic Disc Boundary Detection

Glaucoma is the second most common cause of blindness worldwide. It is characterized by elevated Intra Ocular Pressure (IOP), which leads to damage of optic nerve axons at the back of the eye, with eventual deterioration or loss of vision. Progression of glaucoma is slow and silent leading to changes in the shape and size of the optic disc. Therefore, assessment of optic disc size is an important component of the diagnostic evaluation for glaucoma. This has led to the motivation for the accurate detection of optic disc boundary as it is used to detect and measure the severity of disease.

Difficulty in finding the optic disc boundary is due to its highly variable appearance in retinal images. Classical segmentation algorithms such as edge detection, thresholding, and region growing are not enough to accurately find boundary of the optic disc as they do not incorporate the edge smoothness and continuity properties. In contrast, active contour model represent the paradigm that the presence of an edge depends not only on the gradient at a specific point but also on the spatial distribution. Active contours incorporate the global view of edge detection by assessing continuity and curvature, combined with the local edge strength thus providing smooth and closed contours as segmentation results. These properties make them highly suitable for the optic disc boundary detection application. Active contours are energy minimizing splines and are generally classified as parametric or geometric according to their representation. In the proposed work, the automatic optic disc boundary is detected by fitting an implicit active contour based on geometric model as reported in Li *et al.* 2007. Geometric based model differ from parametric models in the sense that they do not depend much on image gradient and are less sensitive to location of initial contour, thus performs better for object with weak boundaries as in case of optic disc. The following sections provide the details of optic disc boundary segmentation using geometric active contours.

#### A. Elimination of Vessels

The optic disc region is usually fragmented into multiple sub-regions by blood vessels that have comparable gradient values. A homogeneous optic disc region is needed for segmentation using geometric active contour algorithm. Use of median filter with appropriate size to remove interfering blood vessels from the optic disc region resulted in heavy blurring of disc boundaries. Instead a better result is achieved with gray level mathematical morphology to remove irrelevant vessels from the optic disc region.

Gray scale mathematical morphology provides a tool for extracting geometric information from gray scale images. A structuring element is used to build an image operator whose

output depends on whether or not this element fits inside a given image. Shape and size of the structuring element is chosen in accordance with the segmentation task. The two fundamental morphological operations are dilation and erosion. Denoting an image by  $I$  and structuring element by  $S$ , the dilation  $\oplus$  and erosion  $\ominus$  at a particular pixel  $(x, y)$  are defined as

$$(I \oplus S)(x, y) = \max_{i,j} [I(x-i, y-j) + S(i, j)]$$

$$(I \ominus S)(x, y) = \min_{i,j} [I(x+i, y+j) - S(i, j)]$$

where  $i$  and  $j$  index the pixels of  $S$ . The opening of an image is defined as erosion followed by dilation. It tends to smooth the small-scale bright structures in an image. The closing of an image is defined as dilation followed by erosion that tends to smooth the small-scale dark structures in an image and it is given by

$$I \bullet S = (I \oplus S) \ominus S$$

As closing only eliminate image details smaller than the structuring element used. The structuring element is selected such that it covers all possible vascular structures, at the same time preserving the edge of optic disc. In most of the retinal images blood vessels are assumed to be not wider than 15 pixels. Hence, symmetrical disc shaped structuring element of size 15x15 is employed for morphological operation. Figure illustrates the gray scale morphology closing result on typical gray level retinal image. Due to dilation operation the small interfering blood vessels are removed. This results in slight blurring of the input image. Next, erosion is done to restore the boundaries to their former position

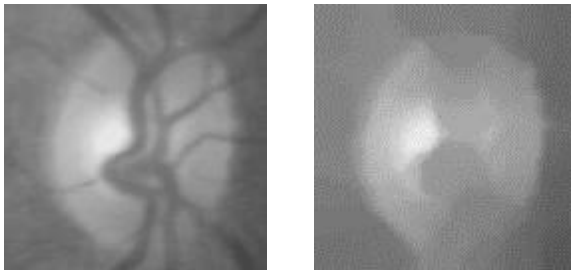


FIGURE 7: Elimination of interfering blood vessels; (a) Optic disc region fragmented by vessels; (b) Morphological closed optic disc region.

*B. Boundary Detection Using Geometric Active Contour Model (ACM)*

In geometric deformation model the curves are evolved implicitly using geometric computations. The evolving curve is represented as level set function  $\phi$  in the image domain  $\Omega$ . Image segmentation is performed by starting with initial curve and evolving its shape by minimizing energy function represented by level set function. The curve evolution has to stop at the image boundaries where the energy is minimum. Here, a contour is represented by zero level set function and the energy function that is to be iteratively minimized to find the object boundary is given as follows.

$$F_{\phi, r_1, r_2} = E_{\phi, r_1, r_2} + \ell P(\phi) + \nu L(\phi)$$

Where  $E_{\phi, r_1, r_2}$  is the external energy function,  $\phi$  is the zero level set representing contour  $C$  in the image domain  $r_1$ , and  $r_2$  are two values that fit the image intensities inside and outside the contour respectively.  $P(\phi)$  is the distance regularizing term used to penalize the deviation of level set from a signed distance function. It is given by

$$P(\phi) = \int_{\Omega} \frac{1}{2} (|\nabla \phi(x)| - 1)^2 dx$$

$L(\phi)$  is the length of zero level curve of used to regularize the contour. It is defined as,

$$L(\phi) = \int_{\Omega} \delta(\phi(x)) |\nabla \phi| dx$$

$\ell$  and  $\nu$  are positive constants,  $\delta$  is the smoothing function called dirac function.

The energy functional is to be minimized to find the optic disc boundary. The gradient descent method proposed by Li *et al.*, 2007 is used to minimize the energy function and it is given as follows:

$$\frac{\partial \phi}{\partial t} = -\delta(\phi)(\alpha_1 e_1 - \alpha_2 e_2) + \nu \delta(\phi) \text{div} \left( \frac{\nabla \phi}{|\nabla \phi|} \right) + \ell \left( \nabla^2 \phi - \text{div} \left( \frac{\nabla \phi}{|\nabla \phi|} \right) \right)$$

The functions  $e_1$  and  $e_2$  are calculated as follows

$$e_1(x) = \int_{\Omega} k_{\sigma}(y-x) |I(x) - r_1(y)|^2 dy$$

$$e_2(x) = \int_{\Omega} k_{\sigma}(y-x) |I(x) - r_2(y)|^2 dy$$

where  $\alpha_1$  and  $\alpha_2$  are positive constants,  $k_{\sigma}$  is the gaussian kernel with localization property with  $\sigma$  as scaling parameter.  $r_1$  and  $r_2$  are two values that fit the image intensities inside and outside the contour. The first term of the equation is called data fitting term responsible for driving the active contour toward object boundary. Second term is called length term and it has smoothing effect on contour. Third term is the level set regularization term that controls the speed of contour. Large value of  $\sigma$  can be used if intensity in homogeneity is not severe. But it increases the computation time with less iterations required for convergence of active contour to boundary. Increasing the value of  $\nu$  introduces emergence of new contours at boundaries of unwanted structures. Therefore, values of  $\alpha_1, \alpha_2, \nu, \ell$  and  $\sigma$  are selected after proper experimentation for the smooth convergence of the active contour to the desired disc boundary.

Once the vascular structures are removed based on the gray scale morphological closing operation, the boundary detection operation is carried out. To fit active contour onto the optic disc the initial contour must be near to the desired boundary otherwise it can converge to the unwanted regions. In order to automatically position an initial contour, the approximate center of optic disc obtained in the localization method is used. A set of points whose distance from the center of optic disc is 50 pixels more than its disc radius are selected. The contour drawn using these points becomes the starting point of the curve. Number of iterations

required to detect the boundary of optic disc varies from image to image. In some images only hundred iterations are enough and in some more than hundred iterations are needed.

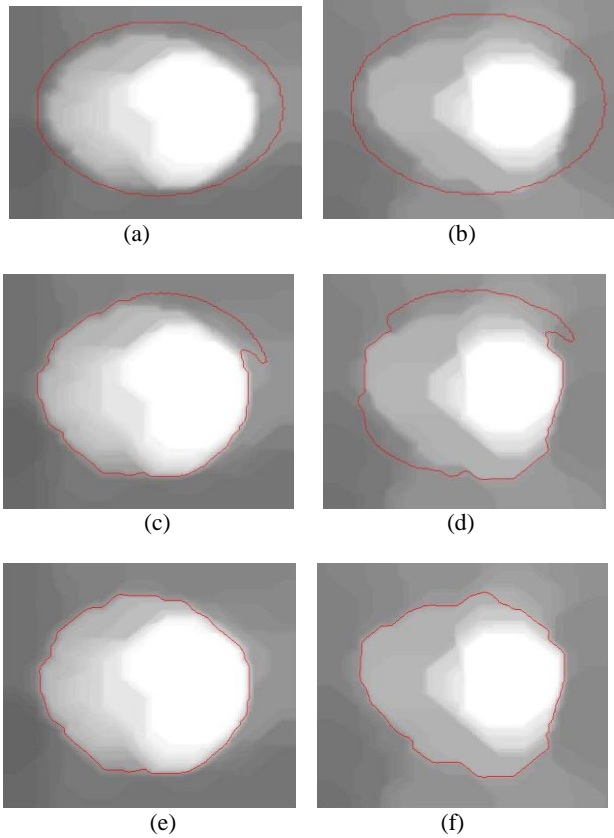


FIGURE 8: of active contour towards optic disc boundary in two different images; (First row) Initial active contour; (Second row) Active contour after 40 iterations; (Third row) Contour after 150 iterations

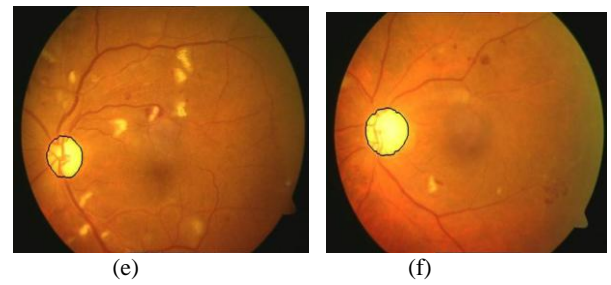
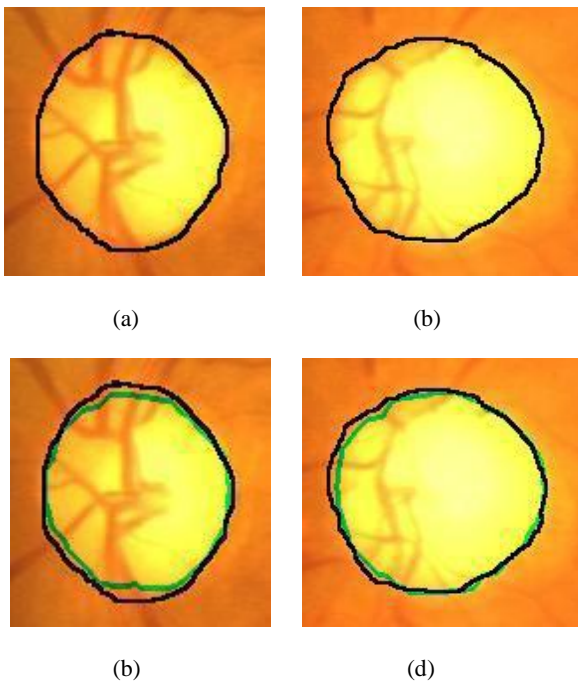


FIGURE 9: Geometric active contour based optic disc boundary segmentation; (a) Hand labeled disc boundary of first image; (b) Hand labeled disc boundary of second image; (c)–(d) Automatically detected boundaries (green colour) overlapped on corresponding hand labeled images; (e) Segmented optic disc boundary with 85% sensitivity; (f) Segmented optic disc boundary with 90.78% sensitivity.

Thus obtained contour specifying the boundary of optic disc is further processed by dilating it with a small structuring element to avoid discontinuities in the contour. The boundary thus detected is compared with the manually marked optic disc boundary by an expert and results are quantified. Figure 5.8 shows the hand labeled optic disc boundary by an expert and automatically detected optic disc boundary overlapped on the ground truth image in different colour.

#### IV. Detection of Macula

The macula is a depression in the center of macular region and appears as a darker area in a colour retinal image. It is located temporal to the optic disc and has no blood vessels present in its center. The fovea centralis lies at the center of the macula that is utilized in activities that require discerning sharp details such as reading. Abnormalities such as exudates present in this region indicate a potential sight threatening condition called maculopathy. The patient may not be aware of the presence of the abnormalities if they are small, but, if left untreated, it results in severe loss of vision. Therefore, it becomes important to detect and mark the macular region in a retinal image for automated detection of abnormalities and their severity level.

In a retinal image, the contrast of macula is often quite low and sometimes it may be obscured by presence of exudates or hemorrhages in its region. Therefore, the macula is localized based on its distance and position with respect to the optic disc as it remains relatively constant. The process of detecting the approximate center and diameter of the optic disc. Once the optic disc is detected, the macula is localized by finding the darkest region within the specified area in the image.

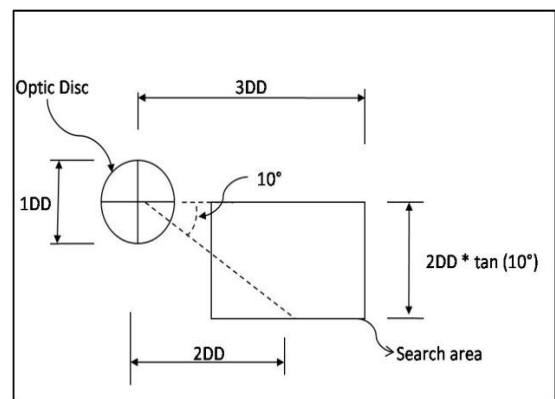


FIGURE 10: Illustration of finding a search area to localize macula

Since the location of macula varies from individual to individual, a rectangular search area has to be defined. In a standard retinal image the macula is situated about 2 disc diameter (DD) temporal to the optic disc. Mean angle between the center macula and the center of optic disc against the horizon is found to be about -5.6 3.3 degrees. Based on this prior knowledge a rectangular search area is formed as shown in Figure 5.9. The width of the search area is taken equal to 2DD as the mean angle between the macula and the center of the optic disc to the horizontal, as mentioned, varies between -2.3 to -8.9 degrees. A small pixel window of size 40×40 is formed to scan the entire area and the average intensity at each pixel location is calculated. The center of the window having the lowest average intensity is taken as the center of the macula. Figure 5.10 shows the result of automatic macula detection method. Once the macula is localized, entire macular region can be determined for detecting the presence or absence of maculopathy.

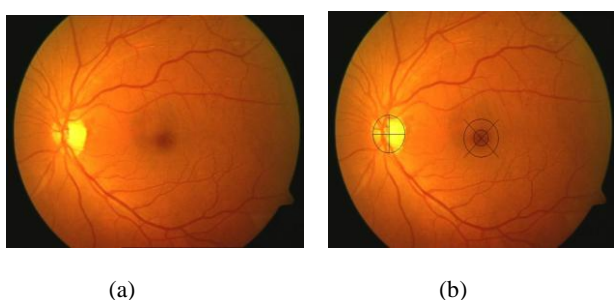


FIGURE 11: Automatic localization of macula; (a) Input retinal image; (b) Marked location of macula and optic disc.

### V. Results and Discussion

For the evaluation of automatic localization of optic disc, segmentation of disc boundary and localization of macula a total of 148 digital colour retinal images from hospital database are used. Out of these 74 images the optic disc boundary are manually drawn by an ophthalmologist as ground truth for disc boundary segmentation method. In optic disc localization, the number of iterations required to calculate the optimal threshold was not more than three for most of the images. The optic disc is located correctly in 147 images out of 148 even in the presence of lesions in the images. For the detection of optic disc boundary initial contour was taken as circle with optic disc center obtained in localization method. All the 74 images were preprocessed with gray morphological closing to eliminate interfering blood vessels. Initial set of points that define contour are automatically selected in the region containing optic disc. As mentioned the size of optic disc diameter in a retina varies from 1.8-2mm (approximately 100 pixels in a standard image). Therefore, a window bigger than this i.e., 150×150 pixels is used to define a region containing optic disc. Several different values were tested for the parameters of the gradient descent flow equation and it was found the weights  $\alpha_1=0.5, \alpha_2=0.5$  that are integrals over the region outside and inside contour as the best for the retinal images. If then it resulted in contour being pulled outwards and if reversed then the contour would converge to regions within optic disc. Value for the length

shortening term  $\nu$  was chosen empirically as 66. Increasing the  $\nu$  resulted in smooth convergence of contour towards disc boundary, but, at the cost of increase in the number of iterations. Scaling parameter  $\sigma$  was set to 2.0 as in some images the optic disc region had intensity in homogeneity. And the regularization value  $\ell$  was set to 1. The number of iterations for convergence of active contour varied from 120 to 200 for different images. Therefore the iteration was set to 200. With these parameter settings the geometric active contour algorithm was applied to 74 images in the dataset. The results were quantified by comparing the segmented disc boundary against the hand labeled ground truth images. Sensitivity is used as the measure to match between two regions in the images. The number of true negatives, that is, the number of pixels not classified as optic disc region pixels, by algorithm is very high. This results in specificity always closer to 100%. All the algorithms were realized using Matlab 7.10 running on 1.66GHz Intel PC with 2GB RAM. And the time taken to detect the optic disc boundary and macula was less than 30 seconds with average sensitivity of  $90.67 \pm 5.05$  for optic disc boundary detection and sensitivity of 96.6% for macula localization.

No. of images	Method	Sensitivity (%)
148	Optic disc localization	99.32
148	Macula localization	96.6
74	Optic disc boundary detection	$90.67 \pm 5.05$

TABLE: Performance of optic disc localization, macula localization and optic disc boundary detection methods

### VI. Summary and conclusion

In this paper, efficient methods for the automatic segmentation of optic disc localization, boundary detection and macula localization in colour retinal images are described. Retinal images of patients at different stages of retinopathy were considered to test the robustness of the optimal iterative threshold method followed by connected component analysis in disc localization. Localization of disc is important as it has to be masked during the exudates detection and its position is used in the location of macula. Based on the result obtained in optic disc boundary detection, it can be stated that geometric based implicit active contour models provide a better segmentation for images with weak boundaries when compared to parametric models. Shape and size changes in optic disc boundaries can be further studied for the detection of glaucoma. The detection of macula and its region plays an important role in the severity level classification of diabetic maculopathy. Detection of all these features leads towards the development of a fully automated retinal image analysis system to aid clinicians in detecting and diagnosing retinal diseases.

Detection of these features of retina was necessary for the proper detection of exudates and also for knowing the severity of the diabetic maculopathy. Based on the fact that optic cup part of the disc being the brightest part in the image, optimal thresholding technique was employed to calculate initial threshold. After experimenting with individual red, green and blue channel of RGB colour image, it was found that gray scale image containing

green channel provide better result when subjected to thresholding. The interfering vessels in the optic disc made the process of finding the approximate center of disc complicated. Fragmented optic disc regions had to be merged to get the center of the disc. According to the prior information about the diameter of optic disc in a standard retinal image, connected components and iterative thresholding was used to locate optic disc. The macula was localized based on its distance and position with respect to the optic disc as it remained relatively constant. Even though macula is considered to be one of the darkest regions without vessels in a retinal image, less contrast between the macula and background makes it difficult to locate based on image variance. Therefore, a rectangular region was formed as a search area to locate the macula in an image. Among 148 images considered for evaluating the methods optic disc and macula were localized with sensitivity of 99.32% and 96.6% respectively.

Detection of optic disc boundary becomes important for the diagnosis of glaucoma. Difficulty in finding the optic disc boundary is due to its highly variable appearance in retinal images. Geometric active contour model was explored to segment the optic disc boundary as classical segmentation algorithms failed to provide good result. Image segmentation was performed by starting with initial curve and evolving its shape by minimizing energy function represented by level set function. The iterative curve evolution was stopped at the image boundaries where the energy was minimum. Experiment was performed on both RGB image and gray scale image and found that implicit active contours provided better result with gray scale images. Total of 74 images were used to evaluate the method. Optic disc boundary drawn manually by an expert was used as ground truth. The method was able to achieve average sensitivity of 90.67% with mean of  $\pm 5.05$ . Based on the result obtained in optic disc boundary detection, it can be stated that geometric based implicit active contour models provide a better segmentation for images with weak boundaries when compared to parametric models.

The changes in the shape and size of optic disc can be used to detect and diagnose sight threatening disease called glaucoma. The method has to be further improved to detect optic cup part of the disc, so that changes in the disc to cup ratio can be used as a measure of glaucoma.

## VII. Reference

- Williams R, Nussey S, Humphrey R, *et al.* Assessment of non-mydratic photography in detection of diabetic retinopathy. *BMJ* 1986;**293**:1140–2.
- Kass M., Witkin A., and Terzopoulos D., —Snakes: active contour models, *International Journal on Computer Vision*, vol. 1, no. 4, pp. 321–331, 1987
- Katz N, Goldbaum M, Nelson M, *et al.* An image processing system for automatic retina diagnosis. *SPIE* 1988;**902**:131–7.
- Ward NP, Tomlinson S, Taylor CJ. Image analysis of fundus photographs. The detection and measurement of exudates associated with diabetic retinopathy *Ophthalmology* 1989; **96**:80–6.
- Chaudhuri S., Chatterjee S., Katz N., Nelson M., and Goldbaum M., —Automatic detection of the optic nerve in retinal images, *Proceedings of the IEEE International Conference on Image Processing*, vol. 1, pp. 1–5. 1989b.
- Taylor R, Lovelock L, Tunbridge WM, *et al.* Comparison of non-mydratic retinal photography with ophthalmoscopy in patients: mobile retinal camera study. *BMJ* 1990;**301**: 1243–7.
- Phillips RP, Spencer T, Ross PG, *et al.* Quantification of diabetic maculopathy by digital imaging of the fundus. *Eye* 1991;**5**:130–7.
- Higgs ER, Harney BA, Kelleher A, *et al.* Detection of diabetic retinopathy in the community using a nonmydratic camera. *Diabetic Med* 1991;**8**:551–5.
- Phillips RP, Spencer T, Ross PGB, *et al.* Quantification of diabetic maculopathy by digital imaging of the fundus. *Eye* 1991;**5**:130–7.
- Retinopathy Working Party. A protocol for screening for diabetic retinopathy in Europe. *Diabetic Med* 1991;**8**:263–7.
- Spencer T, Phillips RP, Sharp PF, *et al.* Automated detection and quantification of microaneurysms in fluorescein angiograms. *Graefes Arch Clin Exp Ophthalmol* 1992;**230**: 36–41.
- Singer DE, Nathan DM, Fogel HA, *et al.* Screening for diabetic retinopathy. *Ann Intern Dis* 1992;**116**:660–71
- Wareham NJ. Cost-effectiveness of alternative methods for diabetic retinopathy screening (letter). *Diabetes Care* 1993;**16**:844.
- Pugh JA, Jacobson JM, Van Heuven WA, *et al.* Screening for diabetic retinopathy. The wide-angle retinal camera. *Diabetes Care* 1993;**16**:889–95.
- Gardner G., Keating D., Williamson T. H., and Elliot A. T., —Automatic detection of diabetic retinopathy using an artificial neural network: a screening tool, *British Journal of Ophthalmology*, vol. 80, no. 11, pp. 940–944, 1996.
- Goldbaum M., Moezzi S., Taylor A., Chatterjee S., Boyd J., and Hunter E., —Automated diagnosis and image understanding with object extraction, object classification, and inferencing in retinal images, *Proceedings IEEE international conference on image processing*, vol. 3, pp. 695–8, 1996.
- Williamson TH, Keating D. Telemedicine and computers in diabetic retinopathy screening (commentary). *Br J Ophthalmol* 1998;**82**:5–7.
- Ibanez M., and Simo A., —Bayesian detection of the fovea in eye fundus angiographies, *Pattern Recognition Letters*, vol. 20, no. 2, pp. 229–240, 1999.
- Hunter A., Lowell, Owens J., and Kennedy L., —Quantification of diabetic retinopathy using neural networks and sensitivity analysis, *Proceedings of Artificial Neural Networks in Medicine and Biology*, Sweden, pp. 81–86, 2000.
- Gagnon L., Lalonde M., and Beaulieu M., —Procedure to detect anatomical structures in optical fundus images, *Proceedings of Conference on Medical Imaging 2001: Image Processing*, vol. 4322, pp. 1218–1225, 2001.
- Goh K. G., Hsu W., Lee Li, and Wang H., —ADRS: An automatic diabetic retinal image screening system, *Medical data mining and knowledge discovery*, Physica-Verlag: Heidelberg, Germany, pp. 181–210, 2001.

22. Facey, K., Cummins, E., Macpherson, K., Reay, L., and Slattery, J., —Organisation of Services for Diabetic Retinopathy Screening: Health Technology Assessment Report 11, Health Technology Board for Scotland, pp. 231-273, 2002.
23. Fong D., Aiello L., Gardner T., and King G., —Diabetic retinopathy, *Diabetes care*, vol. 26, no. 1, pp. 99-102, 2003.
24. Emily Y. C., —Diabetic Retinopathy, *Preferred practice patterns*, American academy of ophthalmology – Retina panel, USA, 2003.
25. Bone H., Steel C., and Steel D., —Screening for diabetic retinopathy, *Optometry*, vol. 6, no. 10, pp. 40-43, 2004.
26. Gonzales R. C., and Woods R. E., —Digital image processing, *2nd Edition, Pearson Education*, pp. 94-101, 2004
27. Chrastek R., Wolf M., Donath K., Niemann H., Paulus D., and Hothorn T., —Automated segmentation of the optic nerve head for diagnosis of glaucoma, *Journal of Medical Image Analysis*, vol. 9, pp. 297–314, 2005.
28. Chang C. I., Du Y., Wang J., Guo S. M., and Thouin P. D., —Survey and comparative analysis of entropy and relative entropy thresholding techniques, *IEE Proceedings of Vision, Image and Signal Processing*, vol. 153, no. 6, pp. 837-850, 2006.
29. Estabridis K., and de Figueiredo R. J. P., —Automatic Detection and Diagnosis of Diabetic Retinopathy, *IEEE International Conference on Image Processing, ICIP*, vol. 2, pp. 445-448, 2007.
30. Fleming D. A., Philip S., Goatman A. K., and Williams J. G., Olson A. J., Sharp F. P., —Automated detection of exudates for diabetic retinopathy screening, *Physics in Medicine and Biology*, vol. 52, no. 24, pp. 7385-7396, 2007.